Millimeter/Submillimeter Wave Communications Via Ceramic Ribbon

C. Yeh, F. Shimabukuro*,
P. Stanton, V. Jamnejad, W. Imbriale, and F. Manshadi
Jet Propulsion Laboratory
California Institute of Technology
4800 Oak Grove Dr., Pasadena, CA 91109

Finding very low loss waveguides in the millimeter/submillimeter wave range has been a problem of considerable interest for many years. Starting from fundamentals, we have found a new way to design a waveguide structure which is capable of providing an attenuation coefficient of less than 10 dB/km for the guided dominant mode. This structure is a ceramic (Coors' 998 Alumina) ribbon with an aspect ratio of 10:1. This attenuation figure is more than one hundred times smaller than that for a typical ceramic or other dielectric circular rod waveguide. It appears that the dominant TM-like mode is capable of "gliding" along the surface of the ribbon with exceedingly low attenuation and with a power pattern having a dip in the core of the ribbon guide. This feature makes the ceramic ribbon to be a true "surface" waveguide structure where the guided wave adheres to a large surface with only a small fraction of the power being carried within the core region of the structure. Here, through theoretical analysis as well as experimental measurements, the existence of this low-loss ceramic ribbon structure is proven. Practical considerations such as the design of an efficient launcher as well as supports for a long open ribbon structure have also been tested experimentally.

The availability of such low loss waveguide may now pave the way for new development in this millimeter/submillimeter wave range.

---

*The Aerospace Corp., El Segundo, CA. 90009

Ever since the discovery by Kao and Hockman [1] that ultra-low-loss optical fiber can be made from pure silica through the elimination of impurities, the ability to guide signals in the optical spectrum with very low attenuation loss is assured. There remains a spectrum from 30 GHz to 300 GHz (called the millimeter/submillimeter (mm/submm) wave band), where low loss waveguides are still unknown. Because of the presence of inherent vibrational absorption bands in solids [2], the elimination of impurities is no longer the solution for finding low loss solids in this spectrum. High skin-depth loss [3] in this spectrum also eliminates the use of highly conducting material. It thus appears that it might be a futile effort to search for ultra-low-loss solids as ultra-low-loss waveguide material in this mm/sub-mm band.

The purpose of this paper is to show a new way to obtain an ultra-low-loss waveguide structure for this mm/sub-mm spectrum band, to show the theoretical foundation for the discovery and experimental verification, to show why such structure is a low-loss structure, and to display its low-loss and power guiding characteristics.

Theoretical Foundation

According to the theory of wave propagation along a dielectric waveguide, the attenuation constant α of a dielectric waveguide surrounded by dry air is given by the following formula [4]:

$$\alpha = 8.686\,\pi\,(1/\lambda_0)\,(\varepsilon_1\, R\, \tan\delta_1) \qquad \text{(dB/m)} \qquad (1)$$

where

$$R = \frac{\int_{A_1} (\mathbf{E}_1 \bullet \mathbf{E}_1^*)\, dA}{(\mu/\varepsilon_0)^{1/2}\left[\int_{A_1} \mathbf{e}_z \bullet (\mathbf{E}_1 \times \mathbf{H}_1^*)\, dA + \int_{A_0} \mathbf{e}_z \bullet (\mathbf{E}_0 \times \mathbf{H}_0^*)\, dA\right]} \qquad (2)$$

Here, ε_1 and tan δ_1 are, respectively, the relative dielectric constant and the loss tangent of the dielectric core material, μ and ε_0 are, respectively, the permeability and permittivity of free-space, λ_0 is the free-space wavelength in meter, $\mathbf{e}_z$ is the unit vector in the direction of propagation, A_1 and A_0 are, respectively, the cross-sectional areas of the core and the cladding region, and $(\mathbf{E}_1,\mathbf{H}_1)$ and $(\mathbf{E}_0,\mathbf{H}_0)$ are, respectively, the modal electric and magnetic field vectors of the guided mode in the core region and in the cladding region. One notes that the attenuation factor α is directly proportional to $\varepsilon_1 R$, defined as the geometrical loss factor. The modal fields of a guided mode on a given guiding structure are governed by the eigen-values and eigen-solutions of the wave equation corresponding to the appropriate boundary conditions [3]. The exact analytic solutions for a dielectric waveguiding structure are only known for a planar dielectric slab, for a circular dielectric cylinder (such as a typical optical fiber) and for an elliptical dielectric cylinder [4]. Numerical techniques [5], such as the finite-element technique, the finite difference time domain technique or the beam propagation technique, must be used for other geometrical shapes. Only hybrid modes with all six field components can be supported by non-circular dielectric waveguides [4].

To find the normal mode solution for arbitrarily shaped dielectric waveguides, an exact approach based on the solution of Maxwell's equations by the finite element method is used. This method has been used successfully to analyze single mode optical waveguides [5]. According to this finite element approach [5], the governing longitudinal fields of the guided wave are first expressed as a functional as follows:

$$
\begin{aligned}
I &= \sum_p I_p \\
&= \sum_p \int\int \Big\{ \tau_p \left|\nabla H_z^{(p)}\right|^2 + \gamma^2 \tau_p \varepsilon_{1p} \left| (\mu/\varepsilon_0)^{-1/2}/\gamma \ \nabla E_z^{(p)} \right|^2 \\
&\qquad + 2\gamma^2 \tau_p \mathbf{e}_z \cdot \left| (\mu/\varepsilon_0)^{-1/2}/\gamma \ \nabla E_z^{(p)} \times \nabla H_z^{(p)} \right| \\
&\qquad - (\omega/c)^2 (\gamma^2 - 1) \left[\left(H_z^{(p)}\right)^2 + \gamma^2 \varepsilon_{1p}/\varepsilon_0 \left[(\mu/\varepsilon_0)^{-1/2}/\gamma \ E_z^{(p)} \right]^2 \right] \Big\} dx\, dy
\end{aligned}
\tag{3}
$$

where

$$\gamma = \beta c/\omega, \qquad \tau_p = (\gamma^2 - 1)/(\gamma^2 - \varepsilon_{1p}) .$$

Here ε_{1p} is the relative dielectric constant in the pth region, β is the propagation constant, ω is the frequency of the wave, $\mathbf{e}_z$ is a unit vector in the z direction, (x,y) are the cross-sectional coordinates, and c is the speed of light in vacuum. The symbol p represents the pth region when one divides the guiding structure into appropriate regions. Minimizing the above surface integral over the whole region is equivalent to satisfying the wave equation and the boundary conditions for E_z and H_z . In the finite element approximation, the primary dependent variables are replaced by a system of discretized variables over the domain of consideration. There, the initial step is a discretization of the original domain into many subregions. For the present analysis, there are a number of regions in the composite cross section of the ribbon waveguide for which the permittivity (dielectric constant) is distinct. Each of these regions is discretized into a number of smaller triangular subregions interconnected at a finite number of points, called nodes. Appropriate relationships can then be developed to represent the waveguide characteristics in all triangular subregions. These relationships are assembled into a system of algebraic equations governing the entire cross section. Taking the variation of these equations with respect to the nodal variable leads to an algebraic eigenvalue problem from which the propagation constant for a certain mode may be determined. The longitudinal electric field, $E_z^{(p)}$, and the longitudinal magnetic field, $H_z^{(p)}$, in each subdivided pth region are also generated in this formalism. All transverse fields in the pth region can subsequently be computed from the longitudinal fields. A complete knowledge of the fields can be used to generate the geometrical loss factor according to Eq. (2). This is the method [5] we used to generate all our theoretical results.

The Geometrical Loss Factor

Examination of the fundamental equation (Eq. (1)) governing the attenuation constant of a dominant mode guided by a simple solid dielectric waveguide surrounded by lossless dry air shows that it is dependent on the loss factor and the dielectric constant of the dielectric material and the geometrical size and shape of the guiding structure [4] [6]. Since the material loss factor and the dielectric constant of a solid are fixed, the only way to reduce the attenuation constant is to find the proper cross-sectional geometry of the waveguide. After performing a systematic study on a variety of geometries, our study

shows that a ribbon shaped guide made with low-loss, high dielectric constant ceramic material, such as alumina, can yield an attenuation constant for the dominant TM-like mode of less than 0.005 dB/m . (Two dominant modes with no cutoff frequency can be supported by this ceramic ribbon structure [4]: a TE-like dominant mode with most of its electric field aligned parallel to the major axis of the ribbon and a TM-like dominant mode with most of its electric field aligned parallel to the minor axis of the ribbon. Sketches of the transverse electric field lines for TE-like, TM-like and HE_{11} modes are given in Fig. 1.) As a comparison, at operating frequency band around 100 GHz, one finds the attenuation constant for the teflon dielectric waveguide at 1.3 dB/m, for the usual metallic rectangular waveguide at 2.4 dB/m, and for the microstripline at 3 dB/m [7]. This remarkable low-loss behavior of a ceramic ribbon guiding the dominant TM-like mode as well as the loss behavior of a ceramic ribbon guiding TE-like mode are shown in Fig. 1 where the geometrical loss factor $\varepsilon_1 R$ is plotted as a function of the normalized cross sectional area $A(\varepsilon_1-1)/\lambda_0^2$. Here, A is the cross-sectional area of the waveguide, ε_1 is the relative dielectric constant of the dielectric guide, and λ_0 is the free-space wavelength. Dielectric ribbons with an aspect ratio of 10 and an alumina circular rod are considered. For the ribbon case, the geometrical loss factors for the dominant TM-like (low-loss) and TE-like (high-loss) modes are obtained for three different dielectric materials: alumina with $\varepsilon_1 = 10$, quartz with $\varepsilon_1 = 4$ and teflon with $\varepsilon_1 = 2.04$. The case for the alumina circular rod supporting the dominant HE_{11} mode is displayed for comparison purposes. It is seen that alumina ribbon supporting the TM-like mode provides the most dramatic reduction in the geometrical loss factor when compared with that for the alumina circular rod. Suitable choice of configuration and dielectric constant can significantly reduce the geometrical loss factor for the TM-like mode. Several important conclusions can be drawn from the results given in Fig. 1:

1. *Dramatically lower geometrical loss factors are obtained for high aspect ratio ribbon waveguide with high dielectric constant. As an example, when the normalized cross-sectional area, $A(\varepsilon_1 -1)/\lambda_0^2$, is 0.4, the geometrical loss factor (as well as the attenuation factor) for this ribbon supporting the dominant TM-like mode is about 140 times smaller than that for a circular rod with the same cross-sectional area supporting the dominant HE_{11} mode.*

2. *To achieve these dramatically lower geometrical loss factors, the guiding structure, supporting the dominant TM-like mode, must be of ribbon shape with high aspect ratio as well as high dielectric constant.*

3. *In the low loss region, i.e., $\varepsilon_1 R < 0.05$, the geometrical loss factor curve for the 10 : 1 ribbon with dielectric constant $\varepsilon_1 = 10$ supporting the TM-like mode is much flatter than that for the circular rod supporting the HE_{11} mode, indicating that the geometrical loss factor for the ribbon is insensitive to small deviations of the normalized cross-sectional area of the ribbon while the geometrical loss factor for the circular rod is very sensitive to size changes in the rod. This means TM-like mode on the ribbon is a very stable mode, not easily disturbed by any geometrical imperfections.*

4. *Separation of the geometrical loss curves for TE-like mode and TM-like mode becomes larger for larger dielectric constant of the guiding ribbon. And, there is a definite relationship between the geometrical loss curves for TE-like mode and that for the TM-like mode. These facts are very significant, because they can be used to devise a fundamentally new way to measure the super low loss characteristics of TM-like mode guided along ceramic ribbon.*

5. *Inspection of the expression for the geometrical loss factor, Eq. (2), shows that the numerator term representing the electric field intensity within the dielectric waveguide governs the magnitude of the geometrical loss factor. To minimize this factor, the electric field intensity must be chosen to be as small as possible over the cross-sectional area of the dielectric guide. It is noted that TM-like mode on a ribbon structure provides precisely this behavior while the opposite is true for TE-like mode on this structure. Thus, TE-like mode yields much higher geometrical loss factor than TM-like mode.*

Experimental Verification

The discovery of the very low geometrical loss factor for the ribbon guiding structure will now be verified by experiments. The most sensitive and accurate way of measuring the attenuation of low loss waveguide is the cavity resonator method. We have successfully developed this method to measure the low attenuation constant of a dielectric waveguide [8]. The resonator basically is composed of a dielectric waveguide placed between two parallel metallic plates with small coupling holes. By measuring the Q of this resonator, one may obtain the attenuation constant of the dielectric waveguide according to the following formula [9]:

$$\alpha = 8.686\,(v_p/v_g)(\beta/2Q)$$

$$= (8.686\pi/Q)\,(v_g/c)\,(1/\lambda_0) \qquad \text{(dB/m)} \qquad (4)$$

where β is the propagation constant of the mode under consideration, v_p is the phase velocity of that mode, v_g is the group velocity of that mode, c is the speed of light in vacuum and λ_0 is the free-space wavelength. Several factors affect the accuracy and sensitivity of this technique: the alignment of the dielectric waveguide with the coupling holes, the alignment of the parallel plates, the uniformity or the straightness of the dielectric

waveguide, the coupling or radiation losses, and the metallic wall losses of the plates. Previous experimental investigation [8] shows that the maximum Q that can be reliably measured by this technique in the Ka band is approximately 30,000. This limits the smallest value of attenuation constant that can be measured.

Let us now examine the relationship between the attenuation constants for TM-like mode and TE-like mode on a dielectric ribbon. From Eqs. (1), (2), (4), one finds

$$\begin{aligned} r_\alpha &= (\alpha_{TE\text{-}LIKE}/\alpha_{TM\text{-}LIKE}) \\ &= (Q_{TM\text{-}LIKE}/Q_{TE\text{-}LIKE})(v_{gTM\text{-}LIKE}/v_{gTE\text{-}LIKE}) \\ &= (\varepsilon_1 R)_{TE\text{-}LIKE}/(\varepsilon_1 R)_{TM\text{-}LIKE} \end{aligned} \tag{5}$$

where $v_{gTE\text{-}LIKE}$ and $v_{gTM\text{-}LIKE}$ are, respectively, the group velocity of the TE-like mode and the TM-like mode, and $Q_{TE\text{-}LIKE}$ and $Q_{TM\text{-}LIKE}$ are, respectively, the Q for TE-like mode and the TM-like mode. The ratio r_α as a function of the normalized cross-sectional area $A(\varepsilon_1\text{-}1)/\lambda_0^2$ for a 10:1 ribbon waveguide for three different ribbon material with ε_1 = 10, 4, 2.04, is shown in Fig. 2. It is seen that for a high dielectric constant ribbon material, such as, $\varepsilon_1 = 10$, the ratio may be quite high, implying that the attenuation for the dominant TM-like mode and that for the dominant TE-like mode can be different by two orders of magnitude. For example, when the normalized area $A(\varepsilon_1\text{-}1)/\lambda_0^2$ is 0.4, r_α is about 88, showing that the attenuation constant for TM-like mode can be 88 times smaller than that for TE-like mode on the same ribbon structure. For the special case of an alumina ribbon with ε_1= 10 and an aspect ratio of 10 having a cross-sectional dimensions of 0.0635 cm (thickness) x 0.635 cm (width), plots of $(Q_{TM\text{-}LIKE}/Q_{TE\text{-}LIKE})$, $(v_{gTM\text{-}LIKE}/v_{gTE\text{-}LIKE})$, $(v_{gTM\text{-}LIKE}/c)$, $(v_{pTM\text{-}LIKE}/c)$, $(v_{gTE\text{-}LIKE}/c)$, and $(v_{pTE\text{-}LIKE}/c)$ vs. frequency are shown in Fig. 3. It is seen that the ratio $(Q_{TM\text{-}LIKE}/Q_{TE\text{-}LIKE})$ for an alumina ribbon can vary from a high of 42 at 30 GHz to 14 at 40 GHz. This means that, for a low loss alumina ribbon with loss tangent = 0.00005, if $Q_{TE\text{-}LIKE}$ is measured at 22,760 at 30 GHz (this Q value is well within the measurement capability our apparatus), $Q_{TM\text{-}LIKE}$ must be 955,900 (this Q value is well beyond the measurement capability of any known room temperature resonant cavity apparatus). To verify this ratio $(Q_{TM\text{-}LIKE}/Q_{TE\text{-}LIKE})$, measurements are made for the

parameters $Q_{TM\text{-}LIKE}$ and $Q_{TE\text{-}LIKE}$ separately using high-loss alumina ribbon to assure that the measured parameters are well within the capability of our apparatus. The high-loss sample is made by coating a 0.0635 cm x 0.635 cm x 11.43 cm low-loss alumina ribbons with a thin layer of carbon particles, such as, dried Indian ink. At 38.8 GHz, $Q_{TM\text{-}LIKE}$ (measured) = 1943 and $Q_{TE\text{-}LIKE}$ (measured) = 123. So, at 38.8 GHz, the ratio, $Q_{TM\text{-}LIKE}/Q_{TE\text{-}LIKE}$ (measured) = 15.79 while $Q_{TM\text{-}LIKE}/Q_{TE\text{-}LIKE}$ (theory) = 15.8. At 32.7 GHz, $Q_{TM\text{-}LIKE}$ (measured) = 5046 and $Q_{TE\text{-}LIKE}$ (measured) = 170. So, at 32.7 GHz, the ratio, $Q_{TM\text{-}LIKE}/Q_{TE\text{-}LIKE}$ (measured) = 29.7 while $Q_{TM\text{-}LIKE}/Q_{TE\text{-}LIKE}$ (theory) = 31. These excellent agreements between measured values and theoretical values, displayed in Fig. 3, show the correctness of the derived theoretical ratio $Q_{TM\text{-}LIKE}/Q_{TE\text{-}LIKE}$. This relationship can now be used reliably to obtain $Q_{TM\text{-}LIKE}$ when $Q_{TE\text{-}LIKE}$ is known.

Using this technique the Q and the attenuation constant for the TM-like mode on ultra-low-loss alumina ribbon is measured. Three batches of alumina material samples were obtained from Coors Ceramic Company [10]. Batch one, made from Coors' Superstrate 996 S20-71 (99.6%, Hirel, Thin Film Substrate), contains ribbons with dimensions 0.0635 cm x 0.635 cm x 11.43 cm. Batch two, made from Coors' extruded 998 Alumina (99.8% Alumina) rectangular rod, contains ribbons with dimensions 0.0635 cm x 0.635 cm x 91.44 cm. Batch three is Coors' extruded 998 Alumina (99.8% Alumina) circular rod with dimensions 0.244 cm (diameter) x 91.44 cm (length). Numerous repeated measurements are made on these samples at various frequencies within the frequency band from 30-40 GHz, using the waveguide resonator technique described above. Typical results are given in the following:

Batch #	Frequency (GHz)	$Q_{TE\text{-}LIKE}$	$Q_{TM\text{-}LIKE}$	α_{TM} (dB/m)	tan δ ($\times 10^{-4}$)
1	38.60	3860±300	64700±4800	0.062±0.005	2.8±0.21
1	32.80	3920±290	121700±9000	0.026±0.002	2.8±0.21
2	38.89	6480±490	103700±7800	0.035±0.003	1.59±0.12
2	32.98	7233±540	216990±16300	0.014±0.001	1.59±0.12
3	39.96	10948±450	10948±450	1.45±0.09	1.0 ±0.04
3	30.03	11117±500	11117±500	1.17±0.08	1.0 ±0.04

The uncertainty in the measured value is due to the causes mentioned previously. Since Batch 3 contains a 91.44 cm long circular Alumina rod, the guiding property of the dominant mode is independent of the orientation of the transverse electric field. Thus, $Q_{TE\text{-}LIKE} = Q_{TM\text{-}LIKE} = Q_{HE}$ for the circular rod. Here Q_{HE} is the Q for the HE_{11} mode on a circular dielectric rod. The importance of the geometrical factor is seen in the measured data. For example, the attenuation constant for an alumina ribbon with aspect ratio of 10 is 0.0096 dB/m at 30 GHz while that for an alumina circular rod with the slightly larger cross sectional area is 1.17 dB/m which is 121 times larger, even though the circular rod is made with less lossy alumina material. That alumina is 30% less lossy than that for the ribbon. The measured data points as well as the calculated results are displayed in Fig. 4. In it the attenuation constant α in dB/m for the low loss dominant mode in various guiding structures is plotted as a function of frequency in GHz in the Ka band. The measured data points refer to alumina rod with diameter 0.269 cm and alumina ribbon with dimensions 0.0635 cm x 0.635 cm. Excellent agreement between the experimental data and theoretical results can be seen. For dielectric waveguides made with either alumina (ε_1=10) or teflon (ε_1 = 2.04), the normalized cross-sectional area of these guides, $A(\varepsilon_1\text{-}1)/\lambda_0^2$, is chosen to be 0.363, where A is the cross-sectional area, ε_1 is the dielectric constant of the guide, and λ_0 is the free-space wavelength. The importance of the geometry of the guide is quite apparent from these curves. For example, at 30 GHz, the alumina rectangular ribbon with aspect ratio of 10 can support a low loss TM-like mode with an attenuation constant at 0.0098 dB/m which is 165 times less than that for the dominant mode on an alumina circular rod with the same cross-sectional area. It is also 61 times less than that for the dominant mode in a standard metallic rectangular waveguide (WR-28). One also notes that a two fold improvement to less than 5 dB/km can easily be obtained for the ribbon if the same alumina material used for the circular rod was used.

Practical Considerations

(a) Experimental Evidence of Guidance by Ceramic Ribbon and Launching Efficiency

To show that guidance is indeed taking place along a ceramic ribbon, we have performed the following experiment: Shown in Fig. 5 are two horns, one transmitting and one receiving, separated by a free-space distance of 86 cm. A 120 ps pulse is emitted from the transmitting horn and is received by the receiving horn as pulse B after traversing

through this free-space distance of 86 cm. Another experiment is performed where a 91.44 cm long ceramic ribbon waveguide with cross-sectional area of 0.0635 cm x 0.635 cm is inserted between the horns. The horns are used to launch and receive the guided wave. Special transitions are used to maximize launching and receiving efficiencies. Launching (or receiving) efficiency of 84% (or loss of less than 0.825 dB) at 39.86 GHz has been measured for an exponential launching horn. The same 120 ps pulse is sent through this ceramic ribbon waveguide structure. The received pulse is labeled as pulse A. The received pulses for these two cases are displayed in Fig. 5. It is seen that the received signal through the ceramic ribbon waveguide is at lease 21 dB greater than that through free space, providing clear evidence that the signal can easily be guided by the ceramic ribbon. The slight delay of the arrival of pulse A also indicates that, due to wave guidance by the alumina ribbon, pulse A is being guided by it and is propagating at the group velocity of the TM-like mode on this structure. This guided group velocity is slower than c, the free-space group velocity, as predicted and as shown in Fig. 3.

(b) Support for the Open Ceramic Ribbon Waveguide

The ceramic ribbon waveguide is an open structure surrounded by dry air. How to support such a structure is an important consideration. One supporting structure appears to be most promising - support made with plastic fish lines. (See Fig. 6.) Thin plastic (low dielectric constant) fish lines, spaced 10.16 cm or longer apart, are strung across wooden rails separated by 5.08 cm (far enough apart so that the exterior guiding field at the ribbon edges has decayed to negligible value). Ceramic ribbon waveguide can simply be laid on top of the fish lines along the middle of the rails. The fish lines can easily support the ceramic ribbon. Any perturbation caused by the fish line support on the propagation characteristics of the guided TM-like mode on the ceramic ribbon waveguide is not detectable.

(c) Joining Sections of Ceramic Ribbon Waveguides

Another problem of practical importance is how to join sections of ceramic ribbon waveguides. We have discovered that a shiplap joint may be used to provide strong bond between two ends of ceramic ribbon. A picture of the shiplap joint is shown in Fig. 6. A quarter inch long of the jointing ribbon end is ground to a thickness of 0.0317 cm which is 1/2 the original thickness of the ribbon. The jointing end of the other ceramic ribbon is prepared similarly. The ends are lapped together, aligned and then glued with "super glue", resulting in a strong bond. No measurable loss due to the joint is found.

Conclusion

A new ultra low loss dielectric waveguide for millimeter/submillimeter waves has been found. It is a high dielectric constant ribbon with dielectric constant of 10 and an aspect ratio of 10:1.

The measured data show that indeed the geometrical factor $\varepsilon_1 R$ of a dielectric waveguide plays a very important role in reducing the attenuation constant of a TM-like mode on a dielectric waveguide provided that the dielectric constant is *high* and the loss tangent is *low* . It is also shown that the dielectric ribbon is the preferred configuration for low-loss guidance. For example, for the same normalized cross-sectional area, say $A(\varepsilon_1 - 1)/\lambda_0^2 = 0.4$, where A is the cross-sectional area of the dielectric waveguide and λ_0 is the operating frequency, the attenuation constant of the dominant TM-like mode on a 10 to 1 aspect ratio ribbon Alumina waveguide is 140 times smaller than that on a circular Alumina rod waveguide, even though the same amount of Alumina material was used to construct these waveguides. (See Figs. 1,4.) The significance of the configuration factor is clear. With the data presented in this paper, this fact has now been verified experimentally.

In conclusion, one notes that the feature of how power is being guided along a high dielectric constant ($\varepsilon_1 = 10$) and the thin ribbon-like structure is instrumental in providing an attenuation constant for the dominant mode of less than 10 dB/km in the 30-300 GHz spectrum range using presently available Coors' 998 Pure Alumina material. The dominant TM-like mode is capable of "gliding" along the surface of the ribbon with exceedingly low attenuation and with a power pattern having a dip in the core of the ribbon guide. This is displayed in Fig. 7. This feature makes the ceramic ribbon to be a true "surface" waveguide structure where the wave is guided along adhering to a large surface with only a small amount of power being carried within the core region of the structure.

Just as the first 20 dB/km optical fiber made in the late 1960s produced a revolution in optical communication, so may the attainment of 10 dB/km ceramic ribbon provide an opening to the 30-300 GHz communication world.

Acknowledgments

We wish to thank Charles Stelzried, Al Bhanji, Dan Rascoe, and M. Gatti of JPL for their enthusiastic encouragement and support. Expert assistance from Richard Cirillo on experimental measurements and from Cynthia Copela in graphic works is greatly appreciated. The research was carried out at the Jet Propulsion Laboratory, California Institute of Technology, under a contract with NASA.

References

1. K. C. Kao and G. A. Hockman, "Dielectric fiber surface waveguides for optical frequencies," Proc. IEE, 133 1151-1158 (1966); G. P. Agrawal, "Fiber Optic Communication Systems," Wiley Series in Microwave and Optical Engineering, New York (1997); D. Marcuse, "Light Transmission Optics", Van Nostrand-Reinhold, New York, NY (1972).

2. M. N. Afsar and K. J. Button, Proc. IEEE 73 131-153 (1985); R. Birch, J. D. Dromey, and J. Lisurf, Infrared Physics 21 225-228 (1981); M. N. Afsar, IEEE Trans. Microwave Theory and Tech. MTT-33 1410-1415 (1985).

3. C. Yeh, "Dynamic Fields", in American Institute of Physics Handbook, 3rd. ed., edited by D. E. Gray, McGraw Hill, New York, NY (1972); S. Ramo, J. R. Whinnery, and T. Van Duzer, "Fields and Waves in Communication Electronics, 2nd. ed., John Wiley Book Co., New York, NY (1984).

4. C. Yeh, "Elliptical Dielectric Waveguides," J. Appl. Phys. 33 3235-3243 (1962); C. Yeh, "Attenuation in a dielectric elliptical cylinder," IEEE Trans. Antenna and Propagation AP-11 177-184 (1963).

5. Numerical Techniques: (1) Finite Element Technique - C. Yeh, K. Ha, S. B. Dong, and W. P. Brown, "Single-Mode Optical Waveguides," Applied Optics 18, No. 10, 1490-1504 (1979). (2) Finite Difference Time Domain Technique - A. Taflove, "Computational electrodynamics, the finite-difference time-domain method," Artech House, Norwood, MA

(1995). (3) Beam Propagation Technique - C. Yeh, L. Casperson and B. Szejn "Propagation of Truncated Gaussian Beams in Multimode Fiber Guides," Journal of the Optical Society of America 68, No. 7, 989-993 (1978).

6. C. Yeh, F. I. Shimabukuro and J. Chu, "Ultra-Low-Loss Dielectric Ribbon Waveguide for Millimeter/Submillimeter Waves," Appl. Phys. Lett. 54 1183-1185 (1989).

7. S. K. Koul, "Millimeter Wave and Optical Dielectric Integrated Guides and Circuits," Wiley Series in Microwave and Optical Engineering, New York (1997).

8. F. I. Shimabukuro and C. Yeh, "Attenuation Measurement of Very Low Loss Dielectric Waveguides by the Cavity Resonator Method Applicable in the Millimeter/Submillimeter Wavelength Range," IEEE Trans. on Microwave Theory and Techniques, 36 1160-1166, (1988).

9. C. Yeh, "A Relation Between α and Q," Proc. IRE 50 2145 (1962).

10. Coors Ceramics Company, Electronic Products Group, 17750 W. 32nd Ave., P.O. Box 4011, Golden, Colorado 80401-0011.

Figure Captions

Fig. 1. The geometrical loss factor $\varepsilon_1 R$ as a function of the normalized cross sectional area $A(\varepsilon_1-1)/\lambda_0^2$. Sketches of transverse electric field lines for the TE-like, the TM-like and HE_{11} modes are also displayed in this figure.

Fig. 2. The ratio r_α as a function of the normalized cross-sectional area $A(\varepsilon_1-1)/\lambda_0^2$ for a 10:1 ribbon waveguide for three different ribbon material with $\varepsilon_1 = 10, 4, 2.04$.

Fig. 3. Ratios of $Q_{TM\text{-}LIKE}/Q_{TE\text{-}LIKE}$, $v_{gTM\text{-}LIKE}/v_{gTE\text{-}LIKE}$, $v_{pTM\text{-}LIKE}/c$, $v_{gTM\text{-}LIKE}/c$, $v_{pTE\text{-}LIKE}/c$, $v_{gTE\text{-}LIKE}/c$ vs. the frequency f (in GHz) for a 10:1 aspect ratio alumina ribbon with dimensions 0.0635 cm x 0.635 cm and dielectric constant $\varepsilon_1 = 10$, supporting the TM-like

mode or the TE-like mode. Measured results are shown as data points. A photo of the Alumina ribbon waveguide resonator is also shown.

Fig. 4. Attenuation constant α in dB/m for the low loss dominant mode in various guiding structures versus frequency in GHz in the Ka band. Measured results are shown as data points; theoretical results are shown as curves.

Fig. 5. Comparison between the received pulses for a 120 ps pulse sent through horns linked by alumina ribbon waveguide and that linked by free-space. Also shown is a picture of a 91.44 cm long single-piece alumina ribbon waveguide with cross-sectional area of 0.0635 cm x 0.635 cm supported by a fish-line supporting section with launching and receiving horns.

Fig. 6. Details of the fishline support and a picture of a section of alumina ribbon with shiplap ends to facilitate the connection between sections of alumina ribbon

Fig. 7. Normalized power intensity distribution for the dominant normal modes (TM-like mode and TE-like mode) on a 10:1 dielectric ribbon structure. Highest power intensity is indicated in red while the lowest power intensity is indicated in blue. The cross-sectional sizes are chosen for single mode operation at 40 GHz.

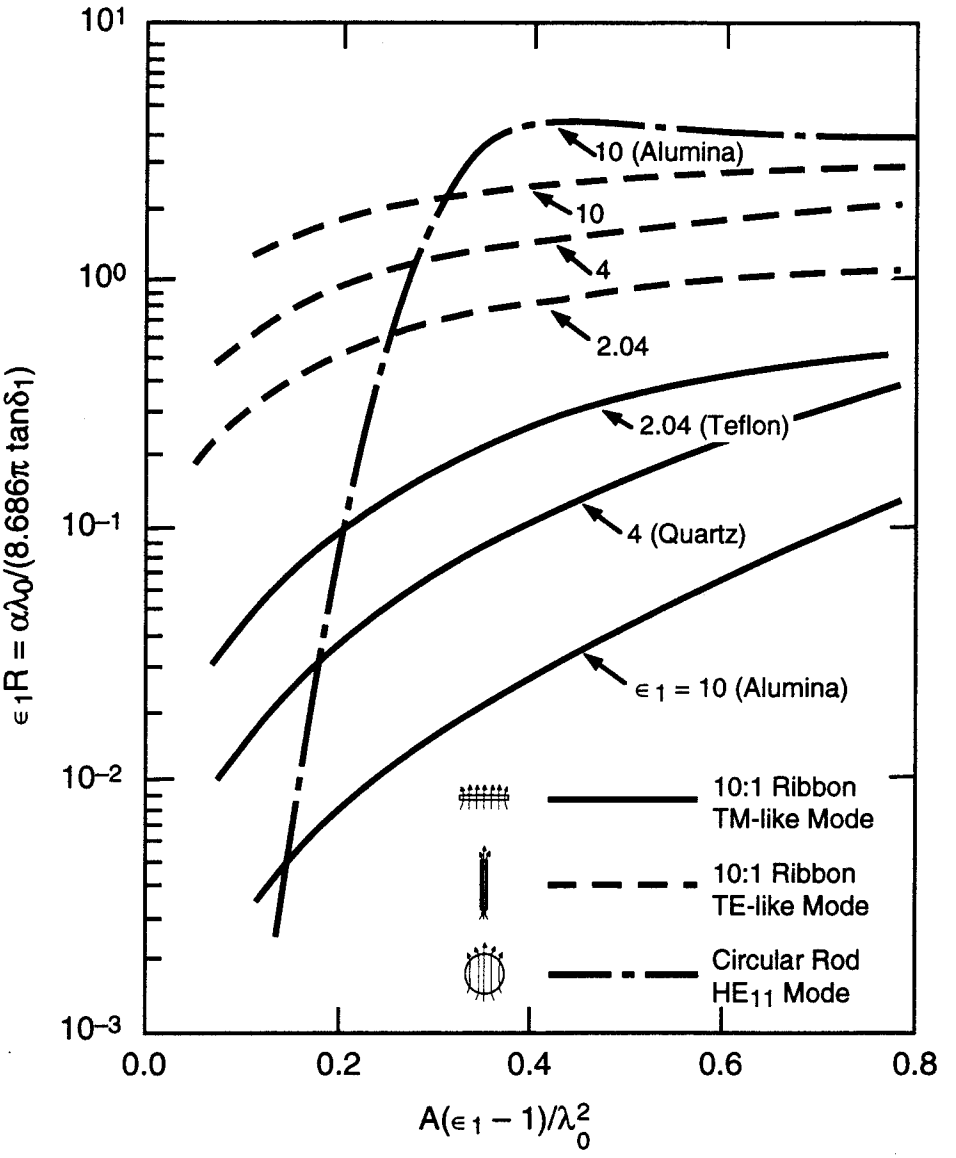

Figure 1. The geometrical loss factor $\varepsilon_1 R$ as a function of the normalized cross sectional area $A(\varepsilon_1-1)/\lambda_0^2$. Sketched in the figure are the transverse electric field lines for the TM-like, TE-like, and HE_{11} mode.

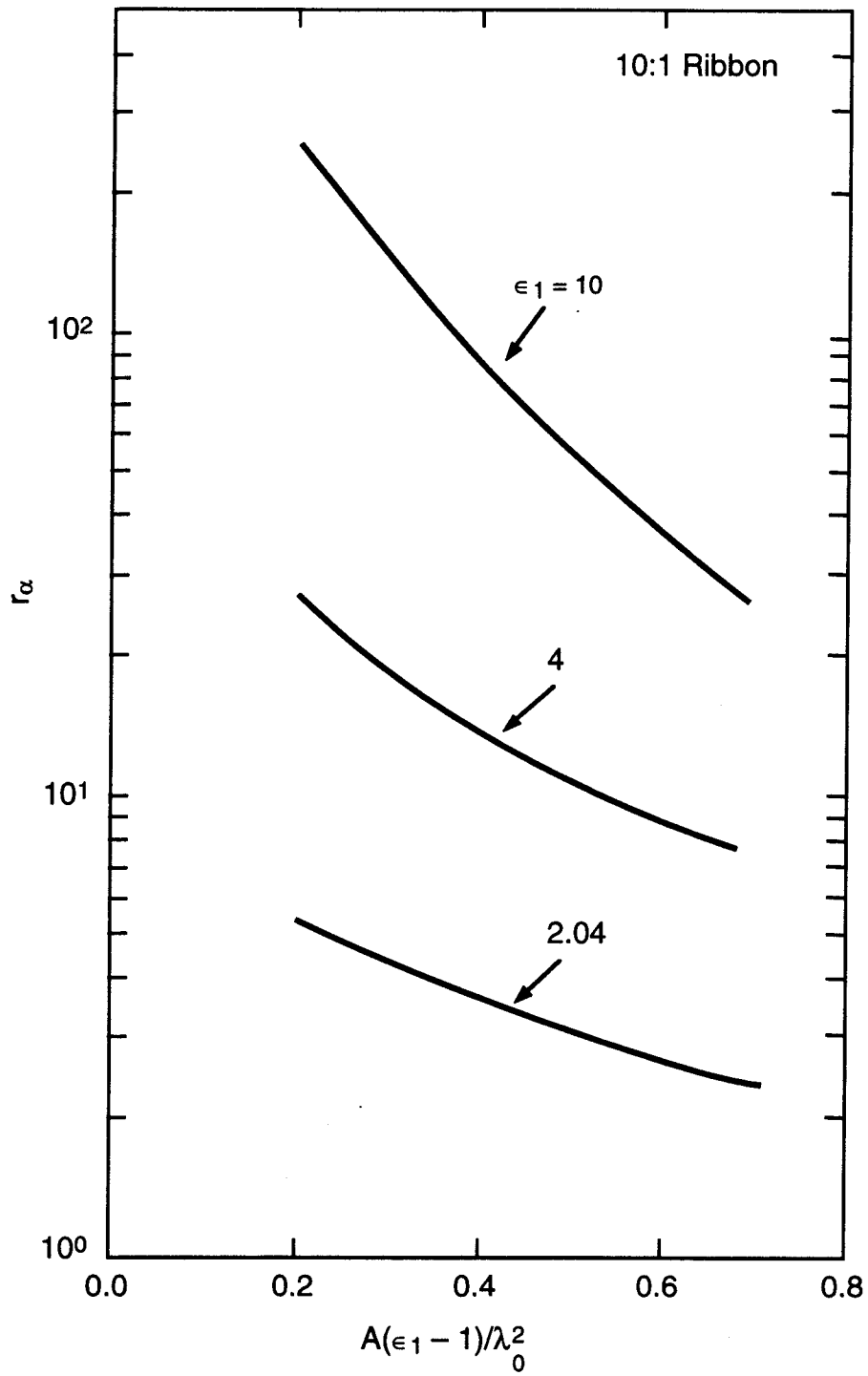

Figure 2. The ratio r_α as a function of the normalized cross-sectional area $A(\varepsilon_1-1)/\lambda_0^2$ for a 10:1 ribbon waveguide for three different ribbon material with $\varepsilon_1 = 10, 4, 2.04$.

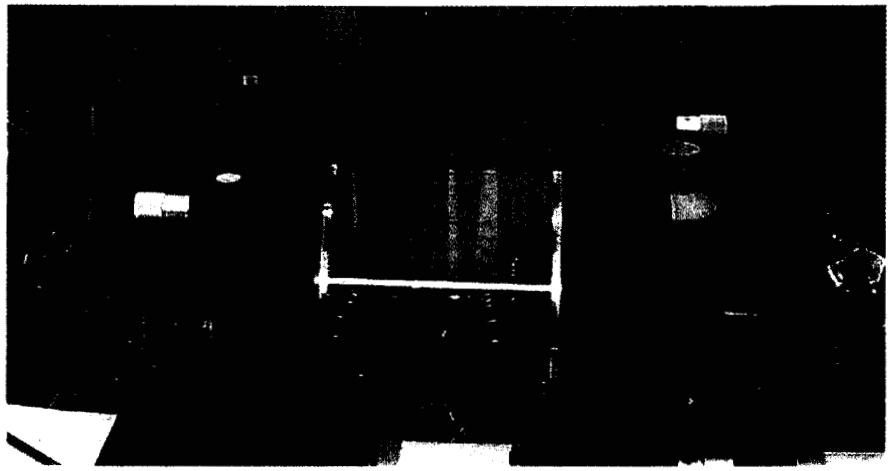

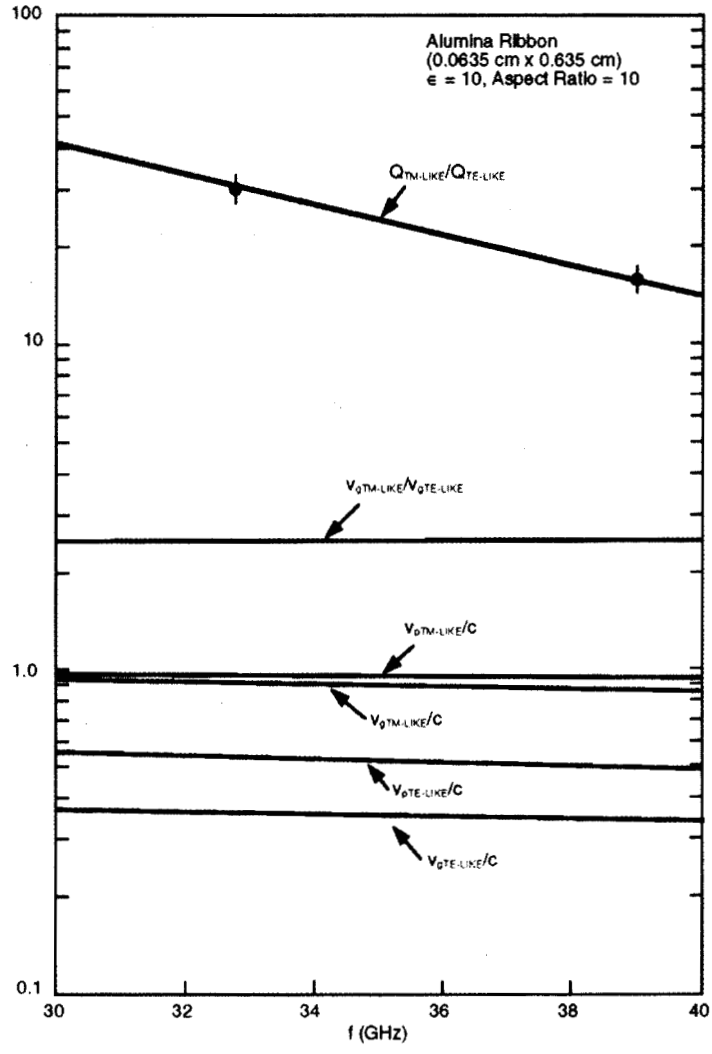

Figure 3. Ratios of $Q_{TM\text{-}LIKE}/Q_{TE\text{-}LIKE}$, $v_{gTM\text{-}LIKE}/v_{gTE\text{-}LIKE}$, $v_{pTM\text{-}LIKE}/c$, $v_{gTM\text{-}LIKE}/c$, $v_{pTE\text{-}LIKE}/c$, $v_{gTE\text{-}LIKE}/c$ vs. the frequency f (in GHz) for a 10:1 aspect ratio Alumina ribbon with dimensions 0.0635 cm x 0.635 cm and dielectric constant $\varepsilon_1 = 10$, supporting the TM-like mode or the TE-like mode. Measured results are shown as data points. A photo of the Alumina ribbon waveguide resonator is also shown.

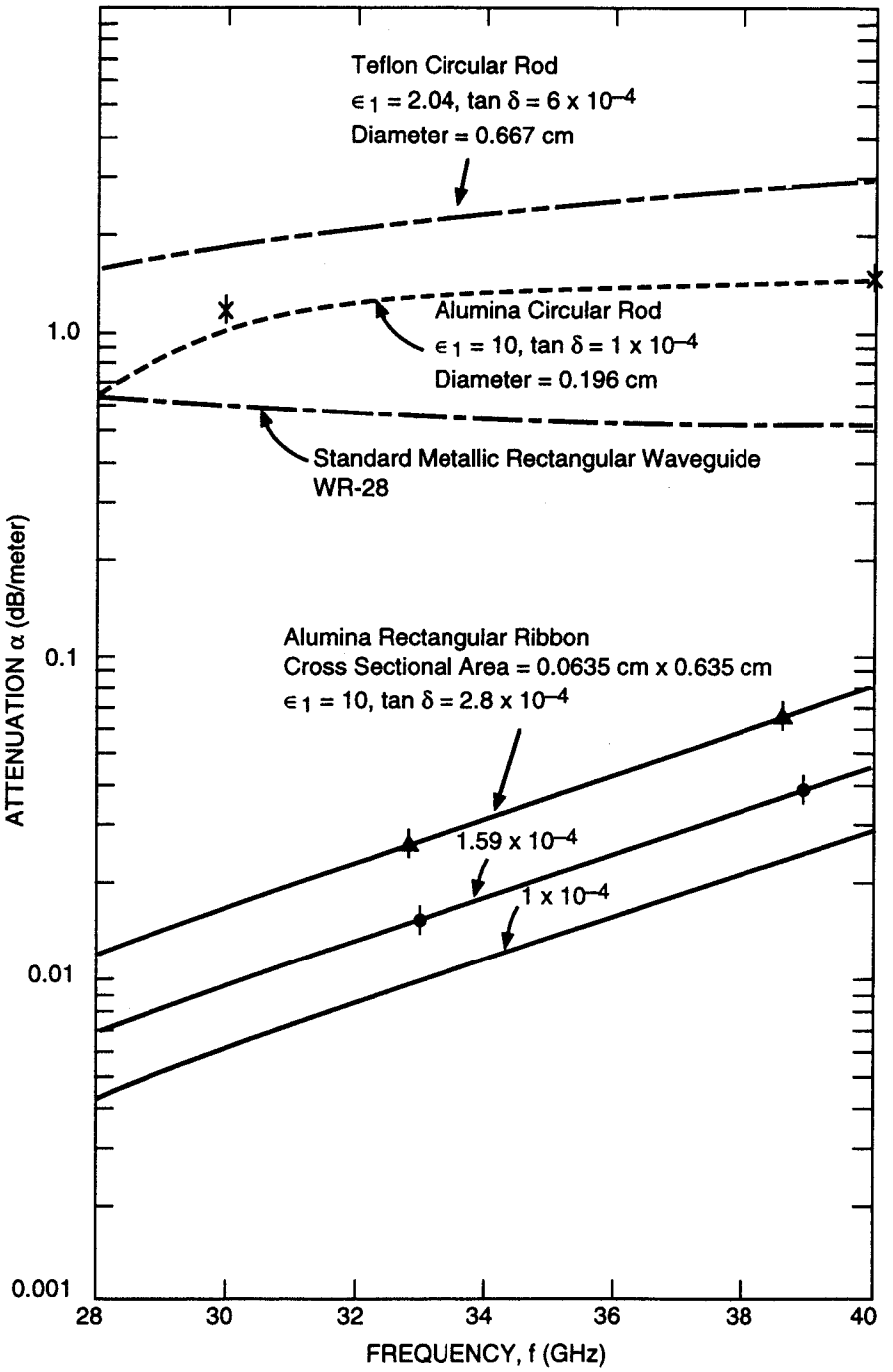

Figure 4. Attenuation constant α in dB/m for the low loss dominant mode in various guiding structures versus frequency in GHz in the Ka band. Measured results are shown as data points; theoretical results are shown as curves.

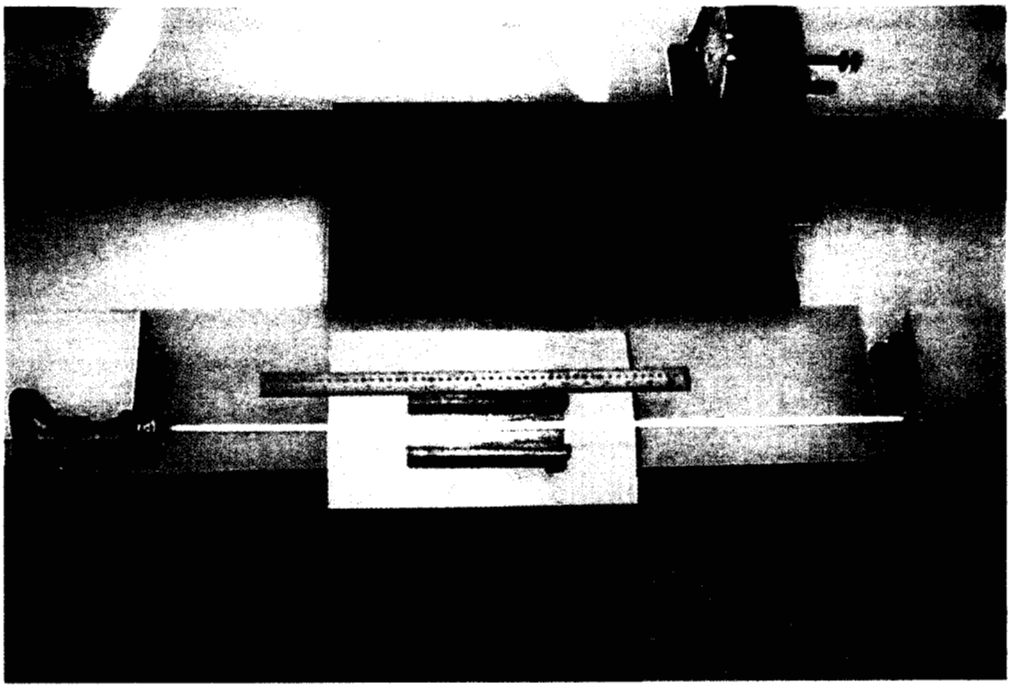

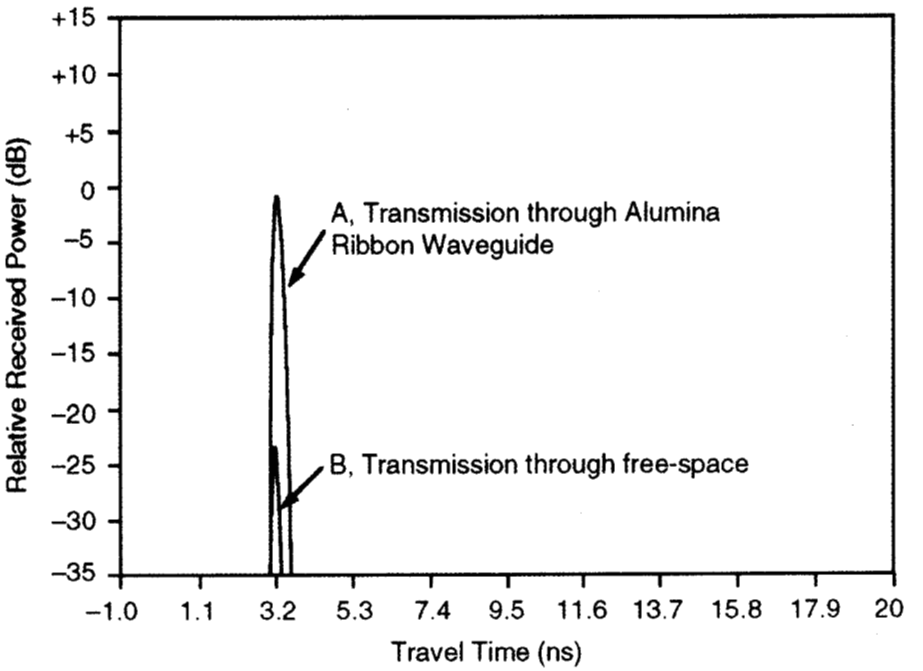

Figure 5. Comparison between the received pulses for a 120 ps pulse sent through horns linked by Alumina ribbon waveguide and that linked by free-space. Also shown is a picture of a 91.44 cm long single-piece Alumina ribbon waveguide with cross-sectional area of 0.0635 cm x 0.635 cm supported by a fish-line supporting section with launching and receiving horns.

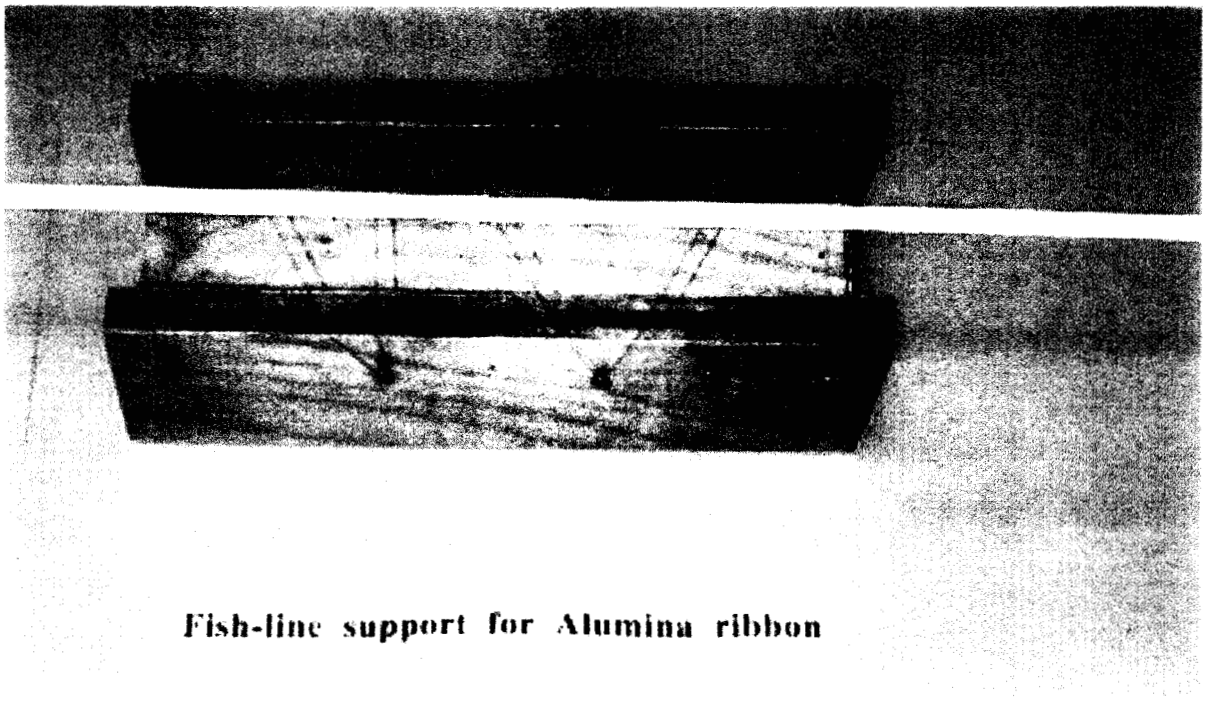

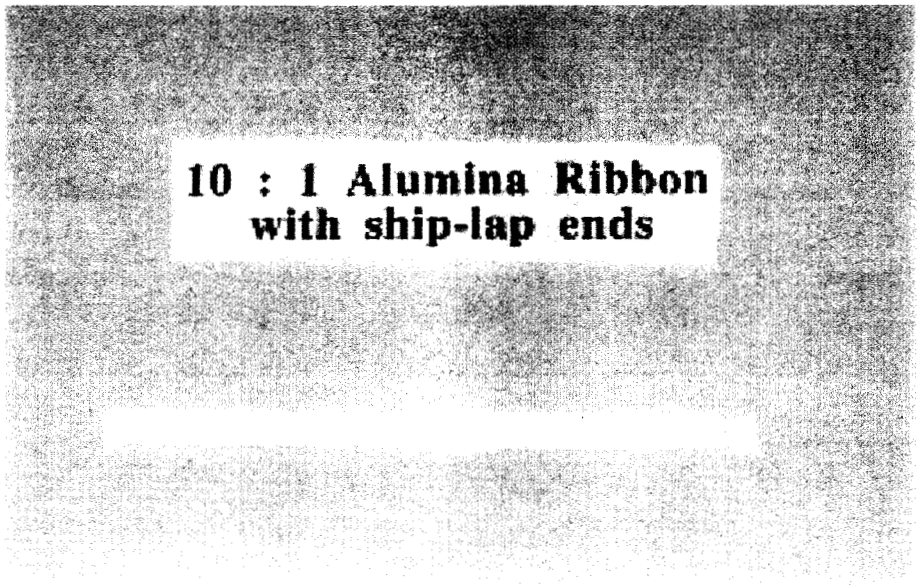

Figure 6. Details of the fishline support and a picture of a section of Alumina ribbon with shiplap ends to facilitate the connection between sections of Alumina ribbon.

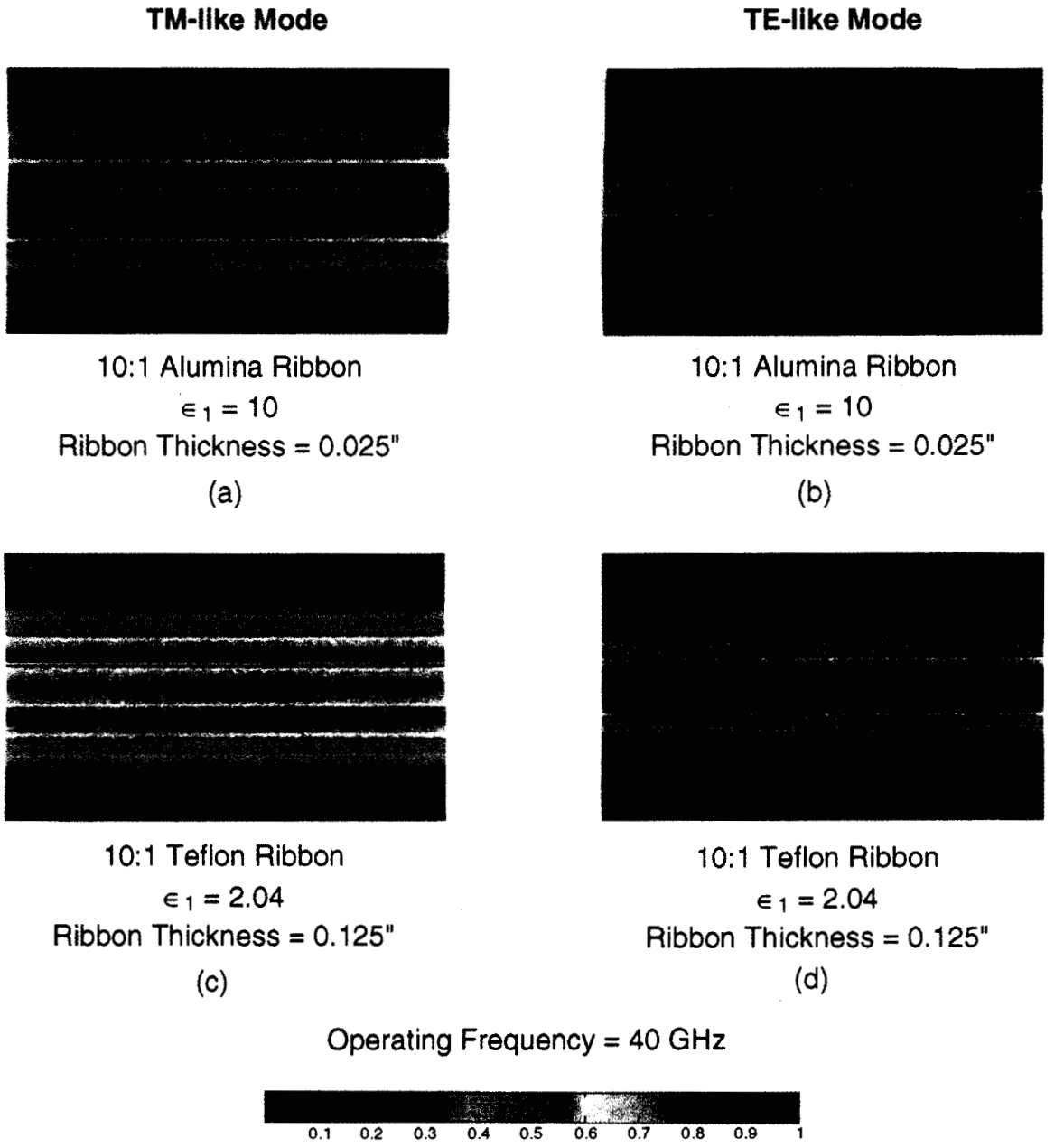

Figure 7. Normalized power intensity distribution for the dominant normal modes (TM-like mode and TE-like mode) on a 10:1 dielectric ribbon structure. Highest power intensity is indicated in red while the lowest power intensity is indicated in blue. The cross-sectional sizes are chosen for single mode operation at 40 GHz.